

## 論文の内容の要旨

### 論文題目: Development of bio-molecular imaging techniques with coherent Raman microspectroscopy

(コヒーレントラマン顕微分光法による生体分子イメージング技術の開発)

氏名: 尾藤 宏達

### Introduction

Time- and space-resolved molecular information on organs, tissues and cells is important in advancing our understanding of life. Broadband multiplex coherent anti-Stokes Raman scattering (CARS) microspectroscopy has enabled fast, quantitative and multi-vibrational mode imaging of tissues and living cells<sup>1</sup>. Although Raman spectrum reflects not only molecular composition but also molecular structures, this strong feature is still underutilized for CARS microspectroscopy. The aim of the present study is to extend CARS microspectroscopy to investigate not only biological molecular compositions but also molecular structures. One approach is development of an analytical method of CARS spectra to extract protein secondary structures. The Another approach is an extension of CARS microspectroscopy with adding a new optical process, coherent Stokes Raman scattering (CSRS).

### 1. Protein Secondary Structure Imaging with CARS microspectroscopy

CARS microspectroscopy provides the third-order nonlinear susceptibility  $\chi^{(3)}$  spectra at high speed. The imaginary part of  $\chi^{(3)}$  spectra corresponds to spontaneous Raman spectra. It is well known that a spontaneous Raman spectrum of a protein in the fingerprint region (intensity, peak position and bandwidth of characteristic bands) sharply reflects its protein secondary structures. Hence, protein secondary structures are visualized through analyzing the retrieved  $\text{Im}[\chi^{(3)}]$  spectra. In this study, a human hair sample as one of the models consisting mainly of proteins is investigated with CARS microspectroscopy.

### Experimental

CARS spectra were obtained from hair samples with and without treatments by chemical reduction and mechanical extension by broadband multiplex CARS microspectrometer<sup>1</sup>.

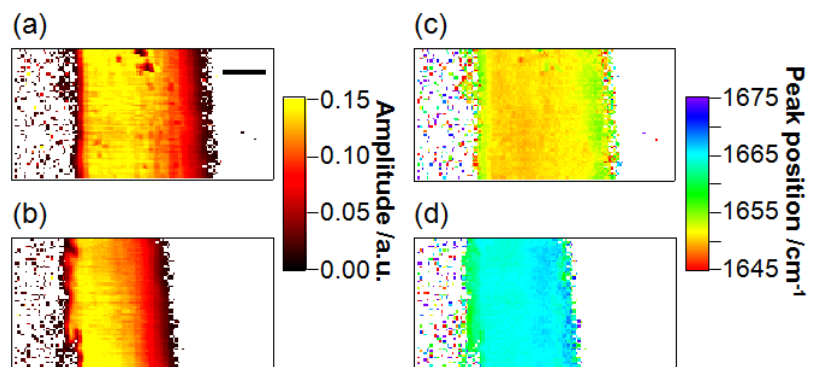


**Fig. 1.** The amide I mode peak amplitude and position images of hair samples; (a) the untreated and (b) the treated hair peak amplitude; (c) the untreated and (d) the treated hair peak position. The scale bar corresponds to 10  $\mu\text{m}$ .

## Results and Discussion

In order to visualize the spatial distributions of protein secondary structures of hairs, two-dimensional intersection images were constructed (see Fig. 1) of the peak amplitude and the peak position of the amide I band observed in  $\text{Im}[\chi^{(3)}]$  spectra. The peak amplitudes did not change between the untreated and treated hairs. On the other hand, the peak positions were dramatically changed between hairs by the phase transition of secondary structures due to the treatments. It clearly visualizes the treatments induced changes in protein secondary structures and their spatial distributions.

## 2. Development of Broadband Multiplex CARS/CSRS Microspectroscopic System

Figure 2 shows the energy diagram of nondegenerate CARS and CSRS with three different laser fields,  $\omega_1$ ,  $\omega_2$  and  $\omega_3$ . Ordinary (degenerate) CARS and CSRS scheme is obtained for  $\omega_1 = \omega_3$ . If a broadband laser source is used as  $\omega_2$ , a broadband Raman coherence is generated. With the third field  $\omega_3$ , broadband CARS and CSRS spectra are produced simultaneously at  $\omega_{\text{CARS}} = \omega_3 + \omega_1 - \omega_2$  and  $\omega_{\text{CSRS}} = \omega_3 - \omega_1 + \omega_2$ . Because the CARS and CSRS spectra do not overlap with each other, they can be detected simultaneously by a multichannel spectrometer.

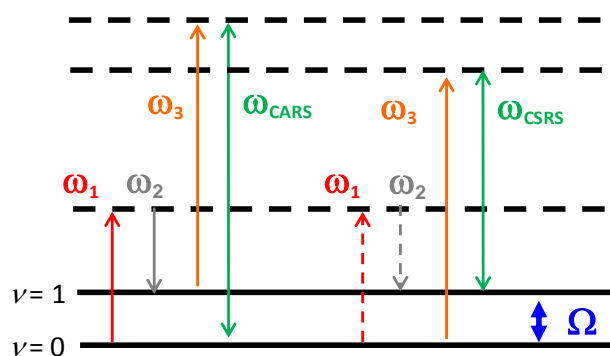


**Fig. 2.** Energy diagram of nondegenerate CARS and CSRS.  $\omega_{\text{CARS}} = \omega_3 + \omega_1 - \omega_2$  and  $\omega_{\text{CSRS}} = \omega_3 - \omega_1 + \omega_2$ .  $\omega_1 - \omega_2 = \Omega$  for a vibrational Raman resonance.  $\nu$  denotes the vibrational quantum number.

## Experimental

The constructed apparatus is schematically shown in Fig. 3. The laser source is a sub-ns microchip Nd:YAG laser, which is also used as a seed laser to generate supercontinuum (SC). The fundamental output (1064 nm), the SC (1.1 ~ 1.7  $\mu\text{m}$ ), and the second harmonic (532 nm) of 1064 nm are used for  $\omega_1$ ,  $\omega_2$ , and  $\omega_3$ , respectively. The coherent Raman signal generated from the sample is spectrally filtered with a dual (532/1064 nm) notch filter. The signal beam is guided into a polychromator, and detected by a CCD camera. The measured CARS/CSRS spectra are intensity-corrected by a non-resonant background from an underneath cover glass measured under the same experimental condition.

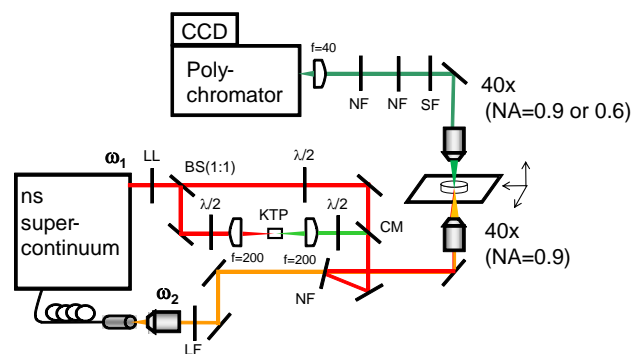


**Fig. 3.** Schematic diagram of the setup of broadband multiplex CARS/CSRS microspectroscopy.

## Results and Discussion

Figure 4 (a) shows a broadband nondegenerate CARS/CSRS spectrum of toluene. The

intensity-corrected CARS spectrum very much resembles the CSRS spectrum, showing that there is no significant electronic resonance effect with  $\omega_3$  at 532 nm. On the other hand, the CARS/CSRS spectrum of 10 mM  $\beta$ -carotene in toluene shows CARS bands much stronger than the corresponding CSRS bands. This asymmetry is due to the electronic resonance of  $\beta$ -carotene, which has a strong electronic absorption at 490 nm. The developed non-degenerate coherent Raman microspectroscopic system enables us to obtain simultaneously the broadband CARS and CSRS spectra with quantitative information on the electronic resonance effect.

### 3. A New Phase Retrieval Method with CARS/CSRS Simultaneous Analysis

The MEM has been recognized as an effective method to retrieve phase information from coherent Raman spectra to obtain  $\text{Im}[\chi^{(3)}]$  spectra that correspond to ordinary Raman spectra<sup>2</sup>. In MEM, an autocorrelation function obtained from a measured coherent Raman spectrum is extrapolated to maximize the information entropy with a fixed maximum lag, the order of pole, as a parameter. The order parameter can be freely selected. Generally, the higher the order is, the better the expected result is, if the measured spectrum contains no noise. Coherent Raman spectra, however, have inevitably non-negligible noise. On the other hand, the lower the order is, the broader the spectral resolution is. Determination of the optimum order of pole without any assumption is desirable in order to extract precise molecular information from coherent Raman spectra in the fingerprint region (intensity, peak position and bandwidth). In this study, I demonstrate a new phase retrieval method through the simultaneous analysis of CARS/CSRS spectra.

#### Experimental

The broadband CARS/CSRS spectrum of a 50 wt% ethanol aqueous solution was measured with the newly developed system. The intensity-corrected spectrum (data points:  $N = 1024$ ) was analyzed with the MEM with an order ( $m < 1024$ ). The  $\text{Im}[\chi^{(3)}]$  spectra obtained from CARS and CSRS are theoretically identical with each other under an electronic non-resonant condition. Therefore, it is expected that the optimum order of pole can be determined through the evaluation of the difference between the retrieved  $\text{Im}[\chi^{(3)}]$  spectra.

#### Results and Discussion

Figure 5 (a) shows the observed CARS/CSRS spectrum of the 50 wt% ethanol aqueous solution. Since ethanol has no absorption in the visible wavelength region, the CARS and CSRS spectra must be

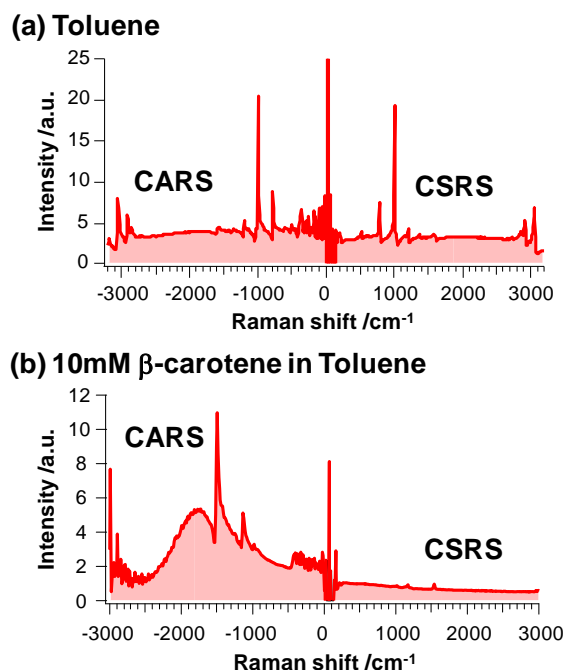
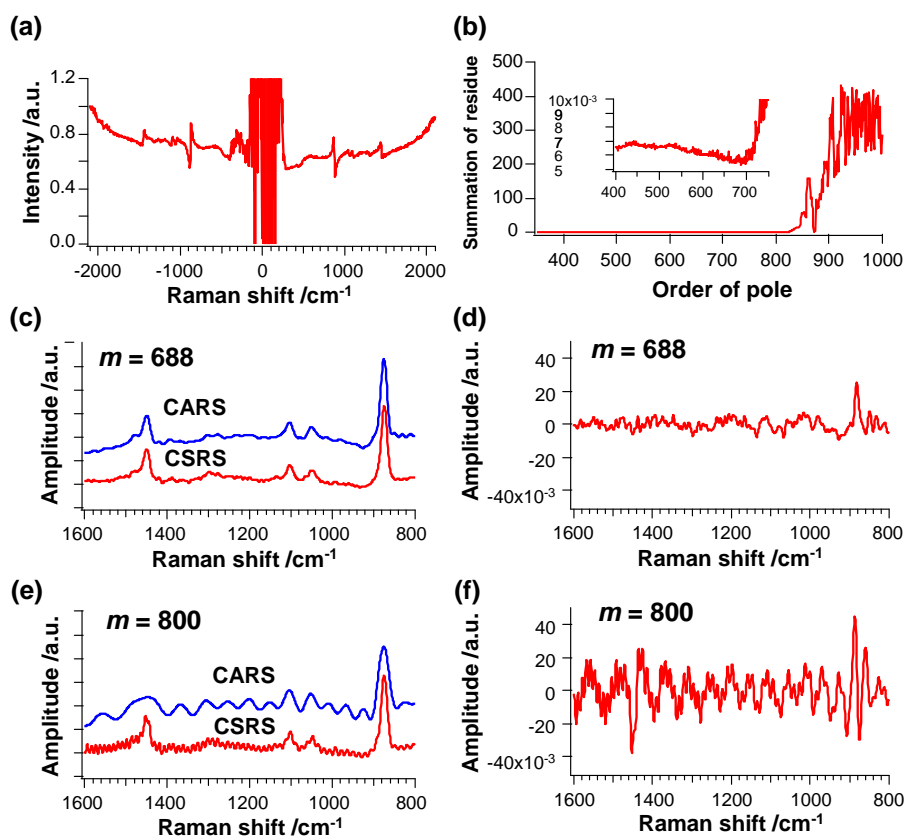


Fig. 4. Broadband multiplex CARS/CSRS spectrum of (a) toluene and (b) 10 mM  $\beta$ -carotene in toluene.

identical with each other. Figure 5 (b) shows the order of pole dependence of the difference between the MEM retrieved  $\text{Im}[\chi^{(3)}]$  spectra obtained from CARS and CSRS. The dependence shows a minimum at  $m = 688$  (see Fig. 5 (b)). In principle, a larger order of pole gives a higher spectral resolution. However, it tends to make the MEM more sensitive to higher frequency noise. Figure 5 (b) therefore shows that 688 is the most appropriate order of pole to make the two  $\text{Im}[\chi^{(3)}]$  spectra from CARS and CSRS consistent with each other, while keeping the highest spectral resolution. The retrieved  $\text{Im}[\chi^{(3)}]$  spectra for  $m = 688$  and their difference are shown in Figs. 5 (c) and (d), respectively.



**Fig. 5.** (a) Intensity-corrected CARS/CSRS spectrum of EtOH aq.; (b) Order of pole dependence of the difference between the  $\text{Im}[\chi^{(3)}]$  spectra obtained from CARS and CSRS; (c) The retrieved  $\text{Im}[\chi^{(3)}]$  spectra for  $m = 688$ ; (d) The difference  $\text{Im}[\chi^{(3)}]$  spectrum for  $m = 688$ ; (e)  $\text{Im}[\chi^{(3)}]$  spectra for  $m = 800$ ; (f) Difference  $\text{Im}[\chi^{(3)}]$  spectrum for  $m = 800$ .

The same data for  $m = 800$  are shown in Figs. 5 (e) and (f). It is obvious that high artificial sharp peaks are generated for  $m = 800$  (Fig. 5 (f)). Thus, the most appropriate order for the MEM is determined to be 688 by using experimental data only. The simultaneous observation of CARS and CSRS spectra with the constructed system provides us with a new reliable phase retrieve method in coherent Raman spectroscopy.

## Conclusion

In this study, the techniques for investigation of bio-molecular structures were developed. They applied to the study of proteins in human hairs, the demonstration of the electronic resonance effect of carotenoids under a microscope and the reliable phase retrieval of CARS spectra of model samples. They will be applied to biological systems for further investigation on roles of bio-molecule structures.

## References

- (1) Okuno, M.; Kano, H.; Leproux, P.; Couderc, V.; Day, J. P. R.; Bonn, M.; Hamaguchi, H. *Angew. Chem. Int. Ed.* **2010**, *49*, 6773-6777.
- (2) Vartiainen, E. M. *J. Opt. Soc. Am. B* **1992**, *9*, 1209-1214.